GEOPHYSICAL RESEARCH LETTERS, VOL. 33, L23106, doi:10.1029/2006GL027110, 2006

Click Here for Full Article

# Timescale for the formation of the cold-dense plasma sheet: A case study

Simon Wing,[1] Jay R. Johnson,[2] and Masaki Fujimoto[3]

Received 5 June 2006; revised 9 September 2006; accepted 2 November 2006; published 9 December 2006.

[1] The timescale for the formation of cold-dense plasma sheet ions was investigated with an event in which the interplanetary magnetic field (IMF) was northward for almost one day. The plasma sheet dawn and dusk flanks appear to reach cold dense states (n > 1 $cm^{-3}$; T < 2 keV) within a few hours after IMF northward turning. Closer to the center (midnight meridian), the ion temperatures reach < 2 keV within a few hours of IMF northward turning, but the ion densities do not reach above 1 $cm^{-3}$ for at least ~8 hours after IMF northward turning. The connection between solar wind ions and plasma sheet cold-component ions is demonstrated. The plasma sheet dawn flank ions appear to lag the solar wind ions by about 3 hours. This study confirms the previous statistical results: (a) the densification of the plasma sheet can be attributed to the influx of the cold-component (magnetosheath/solar wind origin) ions; and (b) the cooling of the plasma sheet can be attributed not only to the influx of the solar wind ions, but also to the cooling of the hot components. Order of magnitude calculations of the plasma sheet filling rate from reconnection and diffusion suggest that both entry mechanisms could result in roughly comparable filling rates. Hence, the dawn-dusk asymmetries would be key in distinguishing the roles of the various proposed entry mechanisms. **Citation:** Wing, S., J. R. Johnson, and M. Fujimoto (2006), Timescale for the formation of the cold-dense plasma sheet: A case study, *Geophys. Res. Lett.*, *33*, L23106, doi:10.1029/2006GL027110.

## 1. Introduction

[2] Satellite observations show that the Earth's plasma sheet ions become cold and dense during periods of northward interplanetary magnetic field (IMF), which has been attributed to the high influx of solar wind/magnetosheath ions [e.g., *Terasawa et al.*, 1997; *Fujimoto et al.*, 1998]. The cold dense plasma sheet (CDPS) typically has ion density ~ >1 $cm^{-3}$ and temperature ~ <2 keV.

[3] Recently, *Wing et al.* [2005] presents the statistical evolutions of the plasma sheet ion densities and temperatures as IMF turned northward and stayed northward for 1 to 10 hours. By separating the cold and hot components, it shows that densification of the plasma sheet can be attributed entirely or almost entirely to the cold-component ions and hence, to the influx of the magnetosheath or solar wind ions. However, the cooling of the plasma sheet ions can be attributed not only to the influx of the magnetosheath ions, but also to the cooling of the hot-component ions.

[4] This paper presents a case study that complements the *Wing et al.* [2005] statistical study. The focus of this case study is an interplanetary magnetic cloud event in which the IMF stays northward for more than 22 hours. During this event, the Geotail satellite was mostly in the plasma sheet and four DMSP satellites, F11, F12, F13 and F14, were operational simultaneously. This event provides an excellent opportunity to study the timescales for the plasma sheet ions to reach a cold-dense state after IMF northward turning and to reach a hot-tenuous state after IMF southward turning. Herein, IMF northward (southward) turning means IMF becoming northward (southward). Together, the present study and our previous statistical study [*Wing et al.*, 2005] provide observational constraints to the competing proposed solar wind particle entry mechanisms.

## 2. Observations

### 2.1. ACE and Wind Solar Wind Observations

[5] The ACE solar wind and IMF observations on 1998 Feb 04–05 near the Langrangian point (L1), approximately $1.5 \times 10^6$ km (~235 $R_E$) upstream of the Earth, are plotted in Figure 1. Although ACE plasma data are not available for Feb 04, ACE IMF data are complete for the entire 2-day event, as shown in Figure 1a. Fortunately, there was another satellite, Wind, that was located near L1 through out this event. During this period, Wind did provide both solar wind and IMF observations, as shown in Figure 1b. Excluding the obvious noises in the Wind data, both Wind and ACE satellites observed similar features.

[6] Figure 1 shows that during this event the IMF Bz behaves in a "sinusoidal" fashion. Initially, the IMF Bz quickly jumps up to near 0 or just slightly negative (southward), then it slowly decreases, reaching ~ −8 nT around Feb 04 12 UT. Then, it slowly increases, crossing 0 just before Feb 04 20 UT. Thereafter, it continues to ascend, maximizing at ~ 6 nT around Feb 05 07 UT before slowly descending and crossing 0 again shortly after Feb 05 18 UT (ACE) or 19 UT (Wind). After that, the IMF Bz stays southward till the end of the event. Note that the IMF is northward for nearly 22–23 hours.

[7] During the northward IMF interval, the velocity slowly decreases from ~330 to ~285 km $s^{-1}$ while the density increases from ~10 to ~30 $cm^{-3}$. There is a density pulse around Feb 05 04 UT that is followed by a period of rapid density increase, before leveling at around 30 $cm^{-3}$.

[1]Johns Hopkins University Applied Physics Laboratory, Laurel, Maryland, USA.
[2]Princeton Plasma Physics Laboratory, Princeton, New Jersey, USA.
[3]Institute of Space and Astronautical Science, Japan Aerospace Exploration Agency, Sagamihara, Japan.

Copyright 2006 by the American Geophysical Union.
0094-8276/06/2006GL027110$05.00

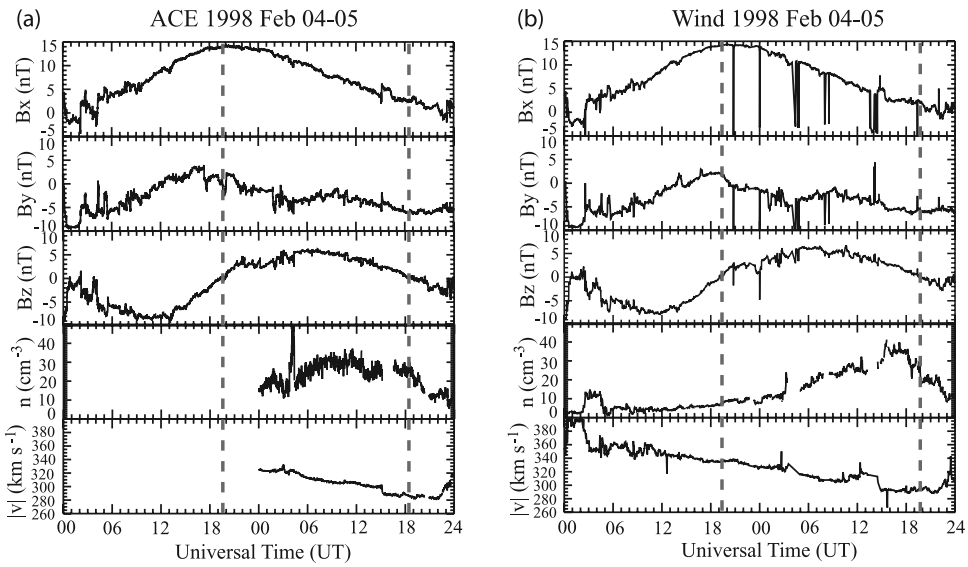


**Figure 1.** The unshifted solar wind and IMF observations at L1 from (a) ACE and (b) Wind. From top to bottom, the panels show IMF Bx, By, Bz, solar wind density, and speed, respectively. The northward IMF interval is between the two dashed vertical lines.

### 2.2. Geotail Observations

[8] Geotail satellite observations during this event are presented in Figure 2. Geotail was located near the equatorial plane traveling from GSM (X,Y,Z) ~ (−30, 4,−3) $R_E$ at the beginning of the event (1998 Feb 04 00 UT) to (−12.5, −15, 0.5) $R_E$ at Feb 05 20 UT, the time of the last data point presented in Figure 2. Prior to Feb 04 15:30 UT, Geotail was mostly in the plasma sheet, but there were intermittent periods when Geotail appeared to be in the lobe, probably resulting from the flapping of the magnetotail that is common during periods of southward IMF. The plasma sheet appears to be hot and tenuous during this interval, typical for southward IMF conditions. Geotail apparently left the plasma sheet between ~15:30 UT and ~19 UT. Upon its return to the plasma sheet, shortly before 19 UT, the plasma sheet still retains its hot-tenuous status, and the spectra look similar to those from the interval before 15:30 UT, as indicated in Figure 2. However, shortly thereafter the Geotail spectra show that the low-energy fluxes begin to increase and the spectra peaks begin to widen, which also coincides with the increasing densities and decreasing temperatures. Toward the end of Feb 04, the spectra exhibit well-formed characteristics that are typical of those of the dawnside plasma sheet during periods of

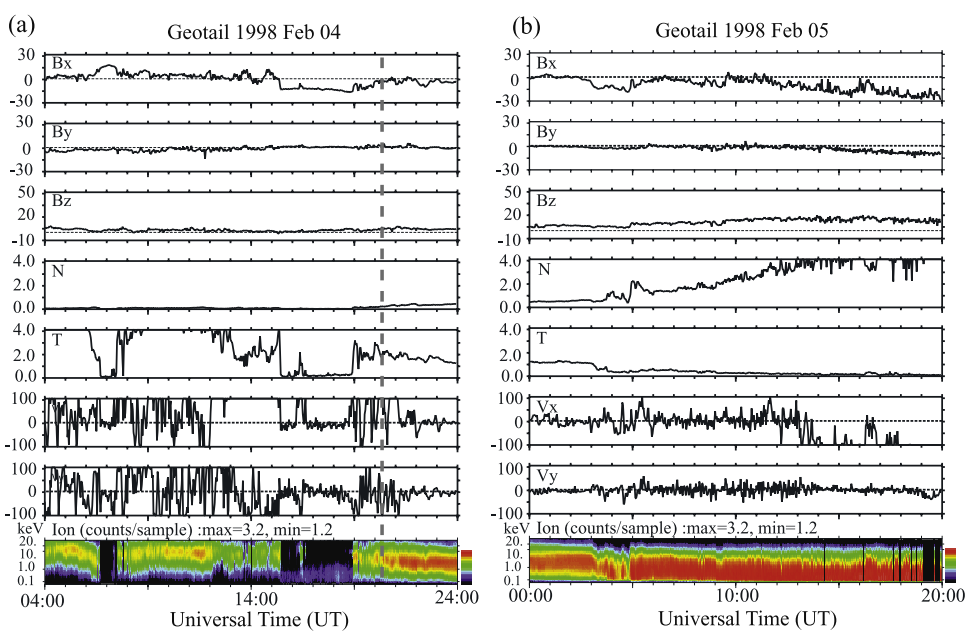


**Figure 2.** Geotail observations on Feb 04–05 1998. The panels show, from top to bottom, Bx, By, Bz, density, temperature, Vx, Vy, and the ion spectrogram. The dashed vertical line marks the IMF northward turning.

northward IMF [e.g., *Fujimoto et al.*, 1998; *Hasegawa et al.*, 2004]. At this time, the plasma densities are still below 1 $cm^{-3}$ and temperatures slightly above 1 keV. The trend of plasma sheet cooling and densification continues on the following day. There appears to be a sharp increase in the densities around Feb 5 05 UT, which can be associated with solar wind density pulse, as discussed in section 3. The densities continue to increase, reaching nearly 4 $cm^{-3}$ while the temperatures reach below 0.5 keV. Just about or shortly before 14 UT, Geotail *Vx* changes from hovering around 0 to $< -100$ km $s^{-1}$, signifying that Geotail has now entered a new region, perhaps the magnetosheath boundary layer or lobe. The latter may result from twisting of the tail due to the significant presence of IMF By at this time [e.g., *Cowley*, 1981].

### 2.3. DMSP Observations

[9] Fortuitously, during this event there were four DMSP satellites operational simultaneously, F11, F12, F13, and F14. Because of its upward pointing and limited pitch-angle resolution, the DMSP SSJ4 instrument measures only highly field-aligned precipitating particles at energy range 32 eV to 30 keV at an altitude of roughly 835 km.

[10] We have developed a method for inferring the plasma sheet ion temperature, density, and pressure from SSJ4 measurements. The method has been described fully elsewhere [*Wing and Newell*, 1998] and is not repeated here. However, for the purpose of the present analysis, some key aspects of the method are reviewed here.

[11] An important aspect of this method is that instead of computing moment, which is widely used, each ion spectrum is fitted to distribution functions (one-component Maxwellian, two-component Maxwellian, and $\kappa$) and the best fit is selected. This takes into account ions outside the detectors' energy range. Therefore, the densities obtained can be larger than those calculated using moments. Moments may also underestimate temperatures by ignoring the hotter components (when they are significant), which may explain some of the temperature differences resulting from using the two methods. An advantage of this method is that when the plasma sheet ions have two components, as they often do during northward IMF [e.g., *Fujimoto et al.*, 1998; *Wing et al.*, 2005], the two components (hot and cold components) can be studied separately.

[12] Using this method and DMSP data, the hourly averaged plasma sheet temperature and density profiles for 1998 Feb 04–05 were constructed. During this event, IMF By fluctuates and its magnitude is at times significant, which may lead to twisting of the tail [e.g., *Cowley*, 1981], complicating the mapping. However, the formation of the cold-dense plasma sheet is a common global phenomenon for northward IMF [e.g., *Øieroset et al.*, 2005] and the present study only extracts macroscale properties from the DMSP observations.

[13] Due to the DMSP orbits, there is a preponderance of data in the dawn and dusk flanks. To track the evolutions of the plasma sheet temperatures and densities, the plasma sheet is divided into two sectors in the Y direction: dawn = $Y < -11$ $R_E$ and dusk = $Y > 11$ $R_E$. Furthermore, in the X direction the plasma sheet is divided into two regions: $X = -10$ to $-25$ $R_E$ and $X = -25$ to $-40$ $R_E$. Figures 3a, 3b, 3c, and 3d plot the evolutions of the temperatures and densities in these four boxes while Figures 3e, 3f, 3g, and 3h plot the evolutions of the cold and hot components of the dawn and dusk sectors for $X = -10$ to $-25$ $R_E$.

## 3. Timescale for the Formation of the Cold-Dense Plasma Sheet Ions

[14] Figure 3 shows that the plasma sheet is initially hot and tenuous during the southward IMF interval. Then, plasma sheet ion densities begin to increase and temperatures begin to decrease shortly before or right after the IMF turns northward. Within a few hours after northward turning, the densities in the flanks appear to reach CDPS status (density > 1 $cm^{-3}$ and temperature < 2 keV). As the IMF Bz continues to stay northward, the densities continue to increase and the temperatures continue to fall. The densities appear to reach a high of 6 $cm^{-3}$ and temperatures appear to drop to about 0.5 keV right around Feb 05 12 UT ($\Delta t \sim$ 36 hours) or $\sim$15 hours after the IMF has become northward. Thereafter, the temperatures appear to stabilize around 0.5 keV, which is very close to the typical magnetosheath ion temperatures. A few hours before the IMF becomes southward, the temperatures begin to increase and densities begin to drop.

[15] Geotail observations appear to follow the same pattern, although there are some differences. Note that unlike the DMSP observations presented in Figure 3, which are for the fixed regions, the Geotail observations were made as the spacecraft moved from just before midnight to the dawn magnetopause. As shown in Figure 2, the densities begin to increase about or slightly before IMF northward turning, while the temperatures appear to decrease about or shortly after IMF northward turning. As the IMF remains northward, the Geotail densities continue to increase, reaching a high of 4 $cm^{-3}$ around Feb 5 12 UT, very close to the time when DMSP densities reach a high. The Geotail temperatures continue to decrease, reaching < 0.5 keV after Feb 5 09 UT, $\sim$12 hours after northward IMF turning. The continuous decline of the temperatures may result from the spacecraft moving closer to the magnetopause. However, DMSP temperatures for both flanks also exhibit a similar trend during the same interval. Moreover, the continuously falling temperature during the prolonged period of northward IMF has also been reported by *Øieroset et al.* [2005].

[16] Within a few hours after IMF northward turning, the Geotail temperatures drop below 2 keV. However, the Geotail densities do not reach above 1 $cm^{-3}$ until Feb 05 05 UT, $\sim$10 hours after northward turning. This is much longer than the timescale for the DMSP densities to reach above 1 $cm^{-3}$. In addition to the factors discussed in section 2.3, the differences could partly be attributed to the locations. Near the time of the northward turning, Geotail made the measurements near the midnight meridian whereas the DMSP densities are for the flanks. The densities in the flanks are typically higher than those near the midnight meridian [e.g., *Terasawa et al.*, 1997]. As expected, the flanks reach the dense state more quickly than the center (near the midnight meridian).

[17] Interestingly, the Geotail observations show that the dawn plasma sheet densities reach a high of 4 $cm^{-3}$ near Feb 05 12 UT, very close to the time when DMSP dawn densities reach a high of 6 $cm^{-3}$ for the region bounded by

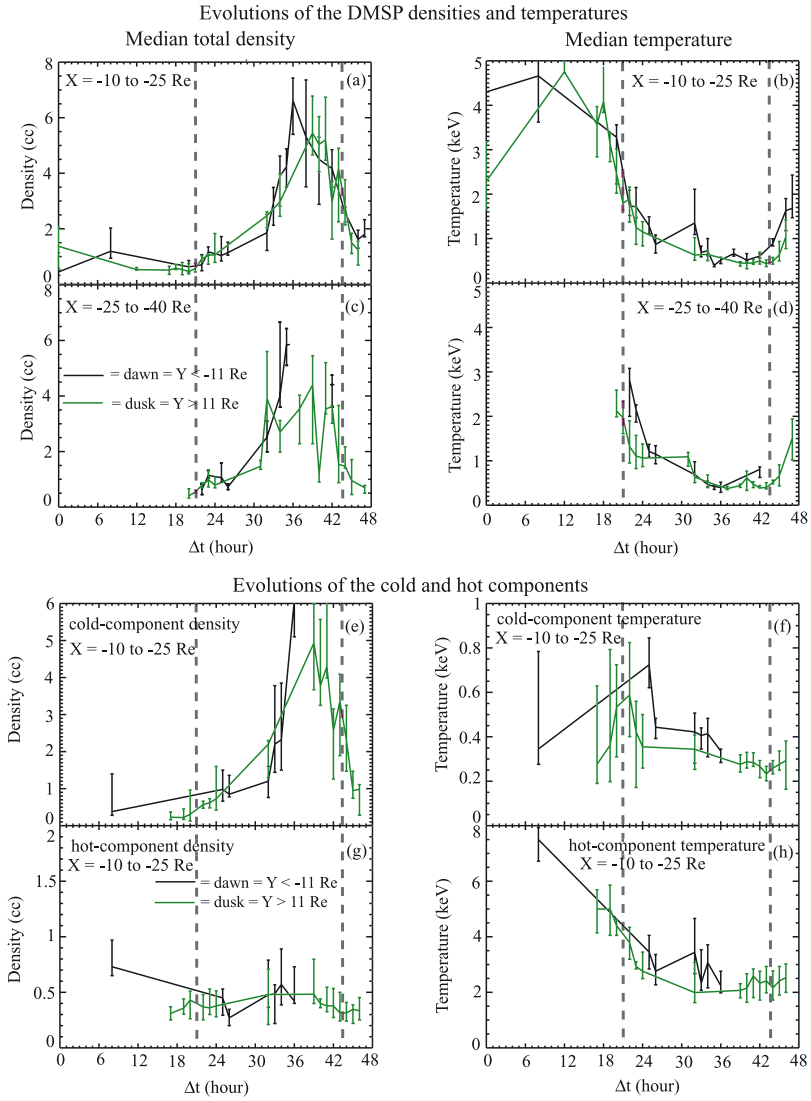


**Figure 3.** (a, b, c, and d) Evolutions of the median densities and median temperatures at the dawn and dusk flanks. Figures 3a and 3b are for X = −10 to −25 $R_E$, whereas Figures 3c and 3d are for X = −25 to −40 $R_E$. (e, f, g, and h) Evolutions of the cold and hot components at the dawn and dusk flanks for X = −10 to −25 $R_E$. The plotted values are the median. The lower and upper error bars indicate the first and third quartiles, respectively. Δt indicates the number of hours since the beginning of the event. For example, Δt = 0 = 1998 Feb 4 00 UT and Δt = 24 = 1998 Feb 5 00 UT. The interval between the first and second dashed vertical lines corresponds to the northward IMF interval.

X = −10 to −25 $R_E$. By this time, Geotail has moved to the dawn flank, the same region measured by DMSP. Again, other than the factors discussed in section 2.3, the density difference here could be partly attributed to the fact that the DMSP densities are averaged in X = −10 to −25 $R_E$ region whereas the Geotail densities come from point measurements at X ∼ −19 $R_E$. The densities typically increase with decreasing distance from the Earth [e.g., *Wing et al.*, 2005], although variations with individual events certainly exist.

[18] Figure 2 shows that Geotail densities appear to sharply increase near Feb 05 05 UT. This can be associated with a solar wind density pulse. Figure 1 shows that ACE observed a solar wind density pulse just after Feb 05 04 UT (unshifted), followed by a period of increasing solar wind densities. Wind only observed the first part of the pulse because of a data gap. The Geotail density jump may not necessarily be linked to the higher solar wind density at this time. It would be expected that this effect could take longer to achieve [e.g., *Terasawa et al.*, 1997; *Borovsky et al.*, 1998]. The higher solar wind densities and hence pressures could change the size and configuration of the magnetosphere more immediately [e.g., *Wing et al.*, 2002] and put Geotail closer to the magnetopause, as evidenced by the transition in the spectra before and after the arrival of the pulse. In fact, the solar wind dynamic pressure changes from 3.4 nPa before the pulse to 4.7 nPa afterward. Unfortunately, there were no DMSP data between Feb 05 04 and 08 UT (Δt = 28–32 hours), but Figure 3 suggests that the plasma sheet dawn densities undergo a big jump between 04 UT (∼ 1cm$^{-3}$) and 08 UT (∼2 cm$^{-3}$).

[19] After the pulse, the solar wind density continuously increases for several hours. In contrast, Geotail densities do

not exhibit a dramatic change in the immediate aftermath of the pulse. In fact, the densities look more or less constant. However, starting around 08 UT, 3 hours after solar wind density begins a rapid increase, the Geotail densities begin to increase at a much higher rate (the slope changes). This density change may result from Geotail entering a high density gradient region. However, sampling the same dawn-side equatorial plasma sheet region, DMSP data show that the densities begin to increase at a higher rate after 08 UT ($\Delta$t ~32 hours) as depicted in Figure 3a, consistent with the Geotail observations. Figures 3e and 3g together suggest that the rapid increase in the total densities can be attributed to the rapid increase in the cold-component ions. This would suggest an increase in the solar wind entry rate, which can be linked to higher solar wind densities with about a 3 hour delay. In comparison, *Borovsky et al.* [1998] reports a 2 hour delay for the solar wind transport to the plasma sheet for an average solar wind condition. The differences may be attributed partly to the slower $\mathbf{E} \times \mathbf{B}$ convection for northward IMF.

[20] An IMF southward turning was observed shortly after Feb 05 19 UT. This is indicated in Figure 3 by the second dashed vertical line, which has taken into account the solar wind propagation. However, the plasma sheet densities begin to decrease and temperatures begin to increase even before the IMF becomes southward, as shown in Figures 3a and 3b. This may result from the fact that the IMF Bz actually begins its slow descent approximately around Feb 05 12 UT, hours before it reaches 0 nT. As IMF Bz gets less northward, IMF By becomes more dominant (the solar wind densities remain relatively stable), which may lead to the increase in the convection [e.g., *Weimer*, 1995], which in turn could increase the (hot and cold) particle losses. In fact, Figures 3e and 3g show that both the hot and cold component dusk densities begin to decrease right around $\Delta$t ~ 39 hours or Feb 05 15 UT (there is lack of data points for the dawn sector at this time).

[21] Finally, Figure 3 shows that after IMF Bz has become completely southward, the temperatures appear to rise much more rapidly. The temperatures reach above 1 keV and densities below 2 $cm^{-3}$ in only a few hours, which can be attributed to the rapid decline of cold-component ions, as shown in Figure 3e.

## 4. Discussion and Summary

[22] In this event, the IMF stayed northward for a prolonged period, more than 22 hours, when Geotail was in the tail and four DMSP satellite were operational, providing a rare opportunity to monitor the formation and evolution of the cold-dense plasma sheet.

[23] The occasionally strong and fluctuating IMF By in this event could introduce additional difficulties to mapping and to the comparisons of the absolute magnitudes of the densities and temperatures in the Geotail and the DMSP observations. However, as long as the properties are macroscale, the relative values of the DMSP observations, e.g., the temperature and density changes, could be used to supplement the Geotail observations to describe the time-scale of the formation of the cold-dense plasma sheet, as demonstrated in section 3.

[24] Figure 3 is similar to the statistical results in Figures 11 and 13 of *Wing et al.* [2005]. For example, during the periods of northward IMF, The densification of the plasma sheet can be attributed almost entirely to the increase in the cold component ions. The cooling of the plasma sheet can be attributed not only to the influx of the cold magnetosheath ions (Figure 3e) but also to the cooling of the hot-component ions (Figure 3h). Figure 3h shows that the temperatures are higher for southward IMF (to the left of first vertical dashed line) than for northward IMF (between the two vertical dashed lines).

[25] It is not clear what causes the cooling of the hot components. It may result from the wave-induced interactions of the cold and hot components and/or expansion of the plasma sheet volume. It may also result from the shortening of the magnetotail as the IMF orientation changes from southward to northward, shortening the distance for adiabatic heating of the hot components that may have originated from more distant locations. If this were the case, then the drop of the temperatures by a factor of 4, from 8 keV ($\Delta$t = 8 hours) to 2 keV ($\Delta$t = 36 hours) (Figure 3h), would suggest that the magnetotail length has been shortened by a factor of 0.6, assuming that $r \; \alpha \; \mathbf{B}^{-3}$, adiabatic invariant, and perfect isotropization.

[26] Several northward IMF solar wind entry mechanisms into the plasma sheet have been proposed. The leading mechanisms include poleward of the cusp reconnections in both hemisphere [e.g., *Song and Russell*, 1992] and diffusive processes, e.g., Kelvin-Helmholtz instability (KHI) [e.g., *Otto and Fairfield*, 2000] and kinetic Alfvén waves (KAW) [e.g., *Johnson and Cheng*, 1997]. Presently, it is not clear which of these mechanisms is dominant. The timescale of the formation of CDPS as well as the dawn-dusk asymmetries provide observational constraints for these various entry mechanisms.

[27] To determine whether one of those mechanisms could be ruled out by the observed entry rate, it is useful to estimate the plasma sheet filling rate due to reconnection and diffusive processes, i.e., KHI and KAW. For northward IMF, particles may enter due to cusp reconnection. Such entry results in ion precipitation with reversed dispersion, as commonly observed by DMSP. If we assume that the open magnetopause is a rotational discontinuity, then there is an inflow across the magnetopause $V_n = V_{An} = \frac{B_n}{\sqrt{\mu_o \rho}}$ where subscript $n$ = the normal component to the magnetopause and $V_{An}$ = the normal component of the Alfvén velocity. The flux per unit area that enters through the open magnetopause is $f_n = n_{sh} \; |V_n| = |B_n| \; \sqrt{\frac{n_{sh}}{\mu_o m}}$, where $n_{sh}$ = magnetosheath density. Then the total entry flux $F$ is given by integrating the flux over the area of the reconnection region on the magnetopause,

$$F = \int_{MP} f_n dA = \int_{MP} |B_n| \sqrt{\frac{n_{sh}}{\mu_o m}} dA.$$

Assuming that the density is roughly constant along the reconnection region on the magnetopause,

$$F \sim \sqrt{\frac{n_{sh}}{\mu_o m}} \int_{MP} |B_n| dA.$$

Because magnetic flux is conserved, the flux may also be evaluated by considering the flux emerging from the cusp region. As the cusp is relatively small (45° longitude and 0.5° latitude) [*Newell et al.*, 1989], the integral may be evaluated as

$$F \sim 2\sqrt{\frac{n_{sh}}{\mu_o m}}|B_{r,c}|R_E^2 \cos\theta_c \ \Delta\theta \ \Delta\phi,$$

where subscript $c$ = cusp, $r$ = the radial component, $\theta_c$ = the cusp latitude (80°), $\Delta\theta$ = the latitudinal extent (0.5 $\pi$/180°), $\Delta\phi$ = the azimuthal extent ($\pi$/4), $B_{r,c} \sim 6 \times 10^{-5}$ T, and the factor 2 is due to the entry occurring at both cusps. For these parameters, there is an influx of $1.2 \times 10^{26}\ n_{sh} 0.5\ s^{-1}$ (in cm$^{-3}$) due to cusp reconnection. Assuming that all these particles are trapped on closed field lines and convected to the plasma sheet without loss, we can estimate an approximate upper-bound filling rate. A simple estimate for the volume of the plasma sheet is a cylinder of radius 15 $R_E$ and length 50 $R_E$ which has volume of $9.3 \times 10^{30}$ cm$^3$ (larger radius would result in larger volume and lower filling rate). Then the mean filling rate would be

$$\frac{\partial n_{ps}}{\partial t} = \frac{F}{V} = \sqrt{n_{sh}}\ 0.046\ \mathrm{cm}^{-3}\ \mathrm{hr}^{-1},$$

where $n_{ps}$ = plasma sheet density, and $n_{sh}$ (in cm$^{-3}$) = magnetosheath density. For the interval in the aftermath of the density pulse, Feb 05 08–12 UT, $n_{sh}$ is assumed to be the observed solar wind $n \sim 30$ cm$^{-3}$. Then, the filling rate is 0.25 cm$^{-3}$ hr$^{-1}$. The observed filling rate is around 0.5 cm$^{-3}$ hr$^{-1}$ for this interval, indicating that reconnection can play a significant role in plasma entry [e.g., *Øieroset et al.*, 2005].

[28] Plasma entry due to diffusive processes may also be estimated. A typical value for the diffusion coefficient D associated with various physical processes is (1–10) $\times$ $10^9$ m$^2$ s$^{-1}$. This value is typical for Kelvin-Helmholtz [*Nykyri and Otto*, 2001], Lower Hybrid Drift [*Winske and Omidi*, 1995], and kinetic Alfvén waves [*Johnson and Cheng*, 1997]. It is useful first of all to consider the extent to which diffusive processes alone could populate the plasma sheet. The timescale for a diffusive process to transport plasma at distance L = 10 $R_E$ is $\tau_D \sim L^2 D^{-1} >$ 100 hours. The inclusion of gradient and curvature drifts would allow more rapid filling, but still on the order of 10 hours. Therefore, it is more likely that if diffusive entry is important and that the entry occurs in a thin layer adjacent to the magnetopause, then the plasma that enters is convected into the plasma sheet by essentially the same processes that redistribute plasma captured on reconnected field lines in the plasma sheet.

[29] To estimate the amount of plasma that can enter due to diffusive entry, we consider a diffusive process that occurs in a diffusive layer $\Delta$ on the inner edge of the magnetopause. For simplicity, consider the diffusive flux through an area A along the magnetospheric flank. The flux entering the diffusive layer is

$$F_A = D\frac{\partial n}{\partial x},$$

where x is the diffusive direction normal to the magnetopause, i.e., GSM Y. If we assume that all the entering plasma is convected and redistributed in a volume A $\times$ $\Lambda$ (that is a CDPS of width $\Lambda$ = 15 $R_E$ in Y direction), then the plasma filling rate is approximately

$$\frac{\partial n_{ps}}{\partial t} \sim \frac{D\delta n}{\Lambda\Delta} \sim 0.3\ \mathrm{cm}^{-3}\ \mathrm{hr}^{-1},$$

where $\Delta$ = 1 $R_E$, $\Lambda$ = 15 $R_E$, $\delta$n = 30cm$^{-3}$, and D = 2 $\times$ $10^9$ m$^2$ s$^{-1}$. It should be noted that the filling rate would initially be larger and then decrease asymptotically to this value as the boundary layer thickens. A larger entry rate could be sustained if the removal of plasma due to convection was significantly faster than the diffusion time. As the observed filling rate is approximately 0.5 cm$^{-3}$ hr$^{-1}$, these observations indicate that diffusive processes can be a significant source for filling the CDPS. One apparent difference in the filling rates for reconnection and for diffusion is the dependence on the magnetosheath/solar wind density (reconnection entry $\sim$ $\mathbf{n}^{0.5}$ vs. diffusive entry $\sim$ $\mathbf{n}$). Of course, care should be taken as the diffusion coefficient could have an additional dependence on density.

[30] Our order of magnitude calculations of the cold, dense plasma sheet filling rates due to reconnection and diffusion suggest that (1) either or both processes may play a significant role in the filling of the plasma sheet and may be complementary; and (2) it would not be easy to distinguish these processes based on just the filling rates—both processes result in comparable entry rates, which are similar to the observed value. Therefore, in order to determine which processes are most important for the filling of the plasma sheet, more attention should be given to the observational signatures of the dawn-dusk asymmetries such as the observed perpendicular heating on the dawn flank population relative to the dusk flank population [e.g., *Hasegawa et al.*, 2003; *Wing et al.*, 2005].

[31] The present study illustrates the power of combining in situ and ionospheric satellites for studying the evolution of the plasma sheet. Studies involving more events similar to the one presented here are planned for the future.

[32] **Acknowledgments.** We would like to acknowledge the assistance of M. Nishino and H. Hasegawa as well as helpful discussions with B. Lavraud. Fred Rich has been helpful in our acquiring DMSP SSJ4 data, as has the World Data Center in Boulder, Colorado. NASA CDAWeb provides the ACE and Wind data. Simon Wing gratefully acknowledges the support of NASA grants NNG04GN14G, NNX06AB87G and NSF grant ATM-0538513. Jay Johnson acknowledges the support of NASA grant NNH04AB23I; and NSF grants ATM-0411392 and ATM-0218847.

## References

Borovsky, J. E., M. F. Thomsen, and R. C. Elphic (1998), The driving of plasma sheet by the solar wind, *J. Geophys. Res.*, *103*, 17,617–17,639.

Cowley, S. W. H. (1981), Magnetospheric asymmetries associated with the *Y*-component of the IMF, *Planet. Space Sci.*, *29*, 79–96.

Fujimoto, M., T. Terasawa, T. Mukai, Y. Saito, T. Yamamoto, and S. Kokubun (1998), Plasma entry from the flanks of the near-Earth magnetotail: Geotail observations, *J. Geophys. Res.*, *103*, 4391–4408.

Hasegawa, H., M. Fujimoto, K. Maezawa, Y. Saito, and T. Mukai (2003), Geotail observations of the dayside outer boundary region: Interplanetary magnetic field control and dawn-dusk asymmetry, *J. Geophys. Res.*, *108*(A4), 1163, doi:10.1029/2002JA009667.

Hasegawa, H., M. Fujimoto, Y. Saito, and T. Mukai (2004), Dense and stagnant ions in the low-latitude boundary region under northward inter-

planetary magnetic field, *Geophys. Res. Lett.*, *31*, L06802, doi:10.1029/2003GL019120.

Johnson, J. R., and C. Z. Cheng (1997), Kinetic Alfven waves and plasma transport at the magnetopause, *Geophys. Res. Lett.*, *24*, 1423–1426.

Newell, P. T., C.-I. Meng, and D. G. Sibeck (1989), Some low-altitude cusp dependencies on the interplanetary magnetic field, *J. Geophys. Res.*, *94*, 8921–8927.

Nykyri, K., and A. Otto (2001), Plasma transport at the magnetospheric boundary due to reconnection in Kelvin-Helmholtz vortices, *Geophys. Res. Lett.*, *28*, 3565–3568.

Øieroset, M., J. Raeder, T. D. Phan, S. Wing, J. P. McFadden, W. Li, M. Fujimoto, H. Rème, and A. Balogh (2005), Global cooling and densification of the plasma sheet during an extended period of purely northward IMF on October 22–24, 2003, *Geophys. Res. Lett.*, *32*, L12S07, doi:10.1029/2004GL021523.

Otto, A., and D. H. Fairfield (2000), Kelvin-Helmholtz instability at the magnetotail boundary: MHD simulation and comparison with Geotail observations, *J. Geophys. Res.*, *105*, 21,175–21,190.

Song, P., and C. T. Russell (1992), Model of the formation of the low-latitude boundary layer for strongly northward interplanetary magnetic field, *J. Geophys. Res.*, *97*, 1411–1420.

Terasawa, T., et al. (1997), Solar wind control of density and temperature in the near-Earth plasma sheet: WIND/GEOTAIL collaboration, *Geophys. Res. Lett.*, *24*, 935–938.

Weimer, D. R. (1995), Models of high-latitude electric potentials derived with a least error fit of spherical harmonic coefficients, *J. Geophys. Res.*, *100*, 19,595–19,607.

Wing, S., and P. T. Newell (1998), Central plasma sheet ion properties as inferred from ionospheric observations, *J. Geophys. Res.*, *103*, 6785–6800.

Wing, S., D. G. Sibeck, M. Wiltberger, and H. Singer (2002), Geosynchronous magnetic field temporal response to solar wind and IMF variations, *J. Geophys. Res.*, *107*(A8), 1222, doi:10.1029/2001JA009156.

Wing, S., J. R. Johnson, P. T. Newell, and C.-I. Meng (2005), Dawn-dusk asymmetries, ion spectra, and sources in the northward interplanetary magnetic field plasma sheet, *J. Geophys. Res.*, *110*, A08205, doi:10.1029/2005JA011086.

Winske, D., and N. Omidi (1995), Diffusion at the magnetopause: Hybrid simulations, *J. Geophys. Res.*, *100*, 11,923–11,933.

M. Fujimoto, Institute of Space and Astronautical Science, Japan Aerospace Exploration Agency, 3-1-1 Yoshinodai, Sagamihara, Kanagawa, 229-8510, Japan.

J. R. Johnson, Princeton Plasma Physics Laboratory, P.O. Box 451, Princeton, NJ 08543-0451, USA.

S. Wing, Johns Hopkins University Applied Physics Laboratory, 11100 Johns Hopkins Road, Laurel, MD 20723-6099, USA. (simon.wing@jhuapl.edu)